

Microoptomechanical pumps assembled and driven by holographic optical vortex arrays

Kosta Ladavac

*James Franck Institute and Dept. of Physics
The University of Chicago, Chicago, IL 60637*

David G. Grier

*Dept. of Physics and Center for Soft Matter Research
New York University, New York, NY 10003*

(Dated: October 29, 2018)

Beams of light with helical wavefronts can be focused into ring-like optical traps known as optical vortices. The orbital angular momentum carried by photons in helical modes can be transferred to trapped mesoscopic objects and thereby coupled to a surrounding fluid. We demonstrate that arrays of optical vortices created with the holographic optical tweezer technique can assemble colloidal spheres into dynamically reconfigurable microoptomechanical pumps assembled by optical gradient forces and actuated by photon orbital angular momentum.

The ever-shrinking scale and increasing complexity of microfluidic systems has created a need for new methods to pump and steer fluids through micrometer-scale channels. Approaches based on hydraulic control [1] and electroosmosis [2] are ideal for many applications and can be implemented flexibly with rapid prototyping methods, and mass-produced with lithographic techniques. They require external control apparatus, however, and are not easily reconfigured in real time. Elegant microfluidic pumps created by driving colloidal particles with actively scanned optical tweezers [3] require *in situ* assembly and so do not lend themselves to low-cost or highly integrated systems.

This Letter describes a new approach to microfluidic control based on the properties of generalized optical traps known as optical vortices [4, 5, 6] that are capable of exerting torques as well as forces. In particular, we employ the recently introduced holographic optical tweezer technique [7] to create arrays of optical vortices that organize fluid-borne colloidal particles into rapidly circulating rings, thereby generating fluid flows with pin-point control and no moving parts.

Our method builds on the insight [8] that helical modes of light carry orbital angular momentum that can be transferred to illuminated objects [9, 10, 11, 12]. Strongly focusing such a beam with a high numerical aperture lens creates a variant of an optical tweezer [13] known variously as an optical vortex, optical spanner, or optical wrench [4, 5, 6]. The necessary helical modes are easily generated from conventional Gaussian TEM_{00} beams with computer-designed diffractive mode converters [4] designed to imprint the helical phase function $\exp(i\ell\theta)$ onto the light's wavefronts. Here, θ is the azimuthal angle around the beam's axis, and ℓ is an integer winding number describing the helix's pitch. Such a beam focuses to a ring of light rather than a bright spot because destructive interference cancels the beam's intensity along its axis. The radius of the dark central core increases

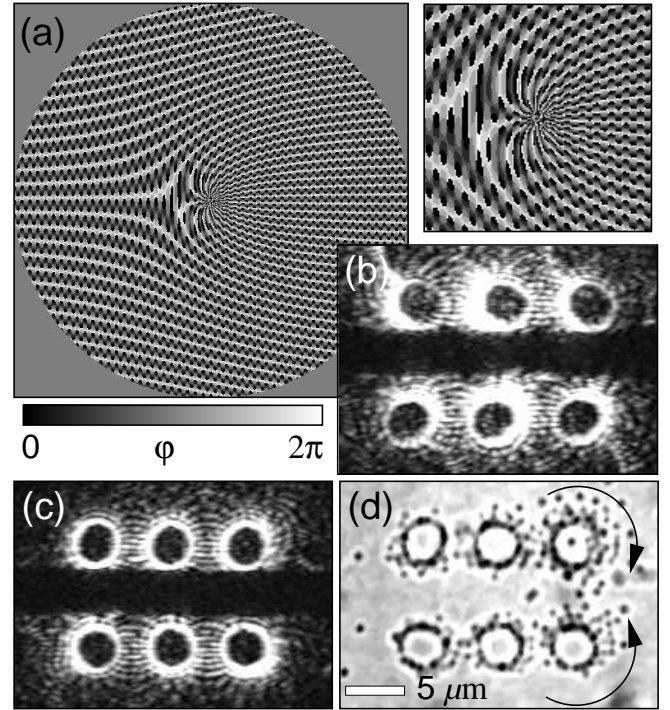


FIG. 1: Creating a microfluidic pump from a beam of light. (a) Gray-scale representation of the phase hologram, $\varphi(\vec{r})$, encoding an optomechanical pump. The color bar translates gray-scale to phase shifts in radians. The inset is an expanded view near the singularity at the optical axis. (b) Focused image of the 3×2 optical vortex array projected by $\varphi(\vec{r})$. (c) The same optical vortex array after aberration correction. (d) Bright-field image of 800 nm diameter silica spheres trapped in the array of optimized optical vortices.

linearly with ℓ [11].

Dielectric objects comparable in size to the wavelength of light are drawn by optical gradient forces toward an optical vortex's bright ring, and are driven around its circumference by the tangential component of the beam's

momentum flux. Colloidal particles dispersed in a viscous fluid can be stably trapped near the focal plane. Their circulation around the ring entrains flows in the surrounding fluid that can be harnessed for controlled transport at extremely small scales.

A single optical vortex does little more than stir a micrometer-scale volume. Arrays of optical vortices, however, can excite larger flows. We create such arrays using the holographic optical tweezer technique [7, 14] in which a computer-generated hologram splits a single laser beam into multiple independent beams, each of which can be focused into a separate optical trap. Each diffracted beam, moreover, can be transformed by the same hologram into a helical mode with an individually specified winding number, ℓ [14]. The phase hologram, $\varphi(\vec{r})$, shown in Fig. 1(a) encodes the 3×2 array of optical vortices whose focal waists appear in Figs. 1(b) and 1(c). The upper row of optical vortices has topological charge $\ell = +21$ and the lower has opposite helicity, $\ell = -21$. The two rows therefore exert torques with opposite senses.

We use a liquid crystal phase-only spatial light modulator (SLM) (Hamamatsu X7550 PAL-SLM) to imprint the trap-forming phase pattern, $\varphi(\vec{r})$, onto the collimated beam provided by a diode-pumped frequency-doubled Nd:YVO₄ laser (Coherent Verdi) operating at $\lambda = 532$ nm. The SLM can selectively shift the light's phase between 0 and 2π radians with 150 calibrated phase gradations at each $40 \mu\text{m}$ wide pixel in a 480×480 array. Positioning the SLM in a plane conjugate to the input pupil of a $100\times$ NA 1.4 S-Plan Apochromat oil-immersion objective lens ensures that each beam diffracted by the phase modulation imposed by the SLM passes through the input pupil and forms an optical trap. The resulting intensity distribution shown in Fig. 1(b) was imaged by placing a mirror in the objective's focal plane and collecting the reflected light with a monochrome CCD camera. A linear spatial filter aligned with the pump's axis in an intermediate focal plane blocks the undiffracted portion of the input beam, which otherwise would create a strong optical tweezer in the middle of the field of view.

Optical vortices are very sensitive to aberrations both in their shape and also in the distribution of light around their circumference. Brightness variations are particularly problematic because particles tend to become localized by optical gradient forces in the brightest regions [11]. As little as $\lambda/10$ of coma can prevent a single particle from circulating around an optical vortex. These distortions are exacerbated in arrays of optical traps created with non-ideal phase masks, so that even a well-aligned optical train results in warped, nonuniform rings such as those in Fig. 1(b). Fortunately, we can correct for the measured aberrations in our optical train [15] by appropriately modifying $\varphi(\vec{r})$. The optimized phase profile combines the functions of a beam-splitter, a mode-

former, and an adaptive optical wavefront corrector and yields the uniform optical vortices in Fig. 1(c), each of which can induce a single particle to circulate freely [11].

We projected this trap array into a colloidal dispersion of 800 nm diameter silica spheres (Bangs Laboratories catalog number SS03N) dispersed in a $12 \mu\text{m}$ thick layer of water between a glass microscope slide and a #1 cover slip. Spheres are drawn to the focal rings and immediately begin circulating, with those in the upper row cycling clockwise and those in the lower row moving counterclockwise. To prevent particles escaping from the rings along the axial direction, we focused the optical vortex array about $h = 2 \mu\text{m}$ below the upper glass surface. A typical snapshot of the optically organized structure appears in Fig. 1(d). This is the first demonstration of motion driven by a heterogeneous array of optical vortices.

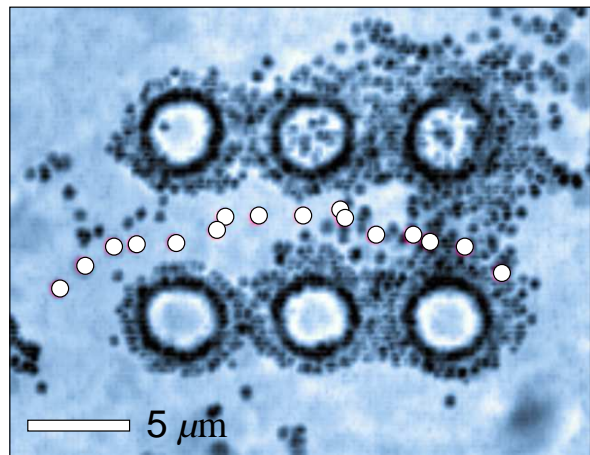


FIG. 2: Time-lapse composite of 16 images in half-second intervals of colloidal spheres in the holographic pump at $P = 2.4$ W. Circles identify the trajectory of a single sphere as it moves $25 \mu\text{m}$ to the left in 7 sec. Its peak speed is $5 \mu\text{m}/\text{sec}$.

Each ring in Fig. 1(d) has a radius of $R = 1.9 \pm 0.1 \mu\text{m}$. The rings' centers are separated by $6.6 \pm 0.2 \mu\text{m}$ in each row, and the rows are separated by $9.1 \pm 0.2 \mu\text{m}$. The entire pattern is centered symmetrically on the optical axis. All of these dimensions, including the position and geometry of the array, are easily changed by appropriately modifying $\varphi(\vec{r})$ [14]. The choice of winding number, $\ell = \pm 21$, was found to optimize the optomechanical efficiency in our apparatus [11].

Coordinated counter-rotation of the two ranks of optically-trapped spheres drives a steady flow from right to left in our images, through the $5 \mu\text{m}$ wide clear channel between the rows, with a return flow outside the pattern. Particles that are not trapped in the optical vortices serve as passive tracers of the fluid flow. Figure 2 shows a multiply exposed image of colloidal spheres' interaction with the optical vortex array. The majority of spheres drawn into the pump's inlet on the right become trapped in the

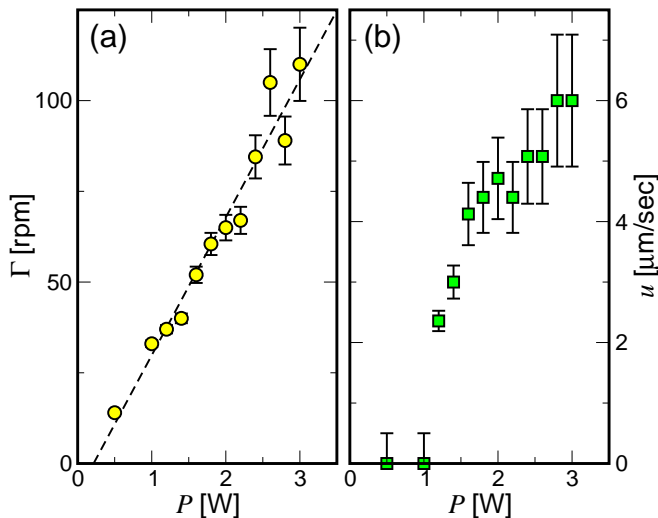


FIG. 3: (a) Circulation rate in revolutions per minute (rpm) and (b) axial flow speed, as a function of laser power.

rings. Some wander into the dark central channel, where they are advected by the flowing water. The circles in Fig. 2 mark the trajectory of one such sphere. We analyzed recorded video sequences to measure the trapped spheres' circulation rate, $\Gamma(P)$, and the flowing spheres' speed, $u(P)$, as a function of laser power. The results appear in Fig. 3.

Each data point in Fig. 3(a) is an average over all six rings, with error bars reflecting both the roughly 5% variation from ring to ring and the estimated 0.05 sec measurement error in the circulation period. The maximum circulation rate, $\Gamma = 1.8 \pm 0.2$ Hz, attained at the highest operating power of our SLM, $P = 3$ W, corresponds to a circumferential speed of $u_0(P) = 22 \pm 2$ $\mu\text{m}/\text{sec}$. No-slip boundary conditions at the spheres' surfaces ensure that the fluid at each vortex's rim also flows at this speed.

The flow field elsewhere in the system can be approximated by the superposition of flow fields due to point forces, known as stokeslets [16], arranged in a ring of radius R at height h below a plane wall. Ensuring that the flow vanishes on the wall requires us to account for the stokeslets' hydrodynamic images in the wall [17]. Accounting for the drag due to the second wall would require a substantially more sophisticated analysis [16, 18] and does not substantially affect the leading-order behavior [19]. The azimuthal component of a single stokeslet ring's wall-corrected far-field flow at radius r from the core and at height h below the wall scales as

$$u(r) = u(R) \left(\frac{R}{r} \right)^2 \quad (1)$$

to lowest order in R/r . We can apply this result to our experimental data by identifying the spheres' observed circumferential speed, $u_0(P)$, with $u(R)$ for spheres substantially smaller than R . This prefactor automatically

includes all optical and drag-induced effects. In the same approximation, the net flow along the channel is the superposition of single-ring flows, with inter-ring coupling also accounted for by $u_0(P)$. Given the arrangement of rings in our system, we anticipate a peak axial flow speed of $u(P) \approx u_0(P)/3$.

We gauge $u(P)$ by tracking particles that wander into the shadow of the linear beam block along the pump's axis. The result, plotted in Fig. 3(b), reaches $u = 6$ $\mu\text{m}/\text{sec}$ at $P = 3$ W, as predicted by Eq. (1). This compares favorably with the performance of actively actuated optical peristaltic pumps [3] and has the added benefit that the pumping structure and its action are all encoded in a single *static* phase pattern that can be implemented with a low-cost microfabricated diffractive optical element.

The comparatively low opto-mechanical efficiency of our implementation can be ascribed to two effects, both of which reflect practical rather than fundamental limitations. The first is the relatively low efficiency of our optical train, in which only 20 percent of the laser power P is actually projected into the sample in the desired mode. The pixellated SLM, furthermore, cannot encode the continuous phase modulation required to create an ideal optical vortex. As a result, the circumference of each ring suffers from an ℓ -fold intensity modulation that establishes a corrugated potential energy landscape [11]. These corrugations deepen as the laser power increases to the point that a single sphere stops circulating altogether. Single-vortex measurements [11] suggest that the pump would stall at $P \approx 12$ W. Below this threshold, the corrugations increase the effective drag on the spheres, and may diminish the circulation rate by as much as 90 percent [11]. Creating holographic microoptomechanical pumps with more refined phase masks in higher-efficiency optical trains therefore should yield substantial efficiency gains.

Loading an optical vortex with multiple spheres offers several benefits for optomechanical drive. Each sphere captures some of the orbital angular momentum flux from the light, and thereby contributes to the linear momentum transferred to the water. Furthermore, collisions among densely trapped spheres helps to minimize the deleterious effects of intensity corrugations and hot spots. Adding too many spheres, however, can jam the pump.

More nuanced and efficient diffractive optical elements would facilitate creating larger and more sophisticated pumping configurations. This suggests opportunities for creating dynamically reconfigured microfluidic systems without physical walls. Also, the chemically synthesized colloidal particles used in our demonstration could be replaced by micromachined gears. Optical vortices trained on the gears' teeth would set them spinning, thereby creating optically driven gear pumps. All of this functionality can be applied to three-dimensional devices by further transforming the helical modes used in this study

into self-healing diffractionless Bessel beams [20, 21].

We are grateful for helpful interactions with Brian Koss and Jennifer Curtis. This work was supported by the National Science Foundation under Grant Number DMR-0304906.

-
- [1] M. A. Unger, H. P. Chou, T. Thorsen, A. Scherer, and S. R. Quake, *Science* **288**, 113 (2000).
- [2] L. Bousse, C. Cohen, T. Nikiforov, A. Chow, A. R. Kopfsill, R. Dubrow, and J. W. Parce, *Annu. Rev. Biophysics Biomolecular Structure* **29**, 155 (2000).
- [3] A. Terray, J. Oakey, and D. W. M. Marr, *Science* **296**, 1841 (2002).
- [4] H. He, N. R. Heckenberg, and H. Rubinsztein-Dunlop, *J. Mod. Opt.* **42**, 217 (1995).
- [5] K. T. Gahagan and G. A. Swartzlander, *Opt. Lett.* **21**, 827 (1996).
- [6] N. B. Simpson, L. Allen, and M. J. Padgett, *J. Mod. Opt.* **43**, 2485 (1996).
- [7] E. R. Dufresne and D. G. Grier, *Rev. Sci. Instr.* **69**, 1974 (1998).
- [8] L. Allen, M. J. Padgett, and M. Babiker, *Progr. Opt.* **39**, 291 (1999).
- [9] H. He, M. E. J. Friese, N. R. Heckenberg, and H. Rubinsztein-Dunlop, *Phys. Rev. Lett.* **75**, 826 (1995).
- [10] A. T. O’Neil, I. MacVicar, L. Allen, and M. J. Padgett, *Phys. Rev. Lett.* **88**, 053601 (2002).
- [11] J. E. Curtis and D. G. Grier, *Phys. Rev. Lett.* **90**, 133901 (2003).
- [12] M. E. J. Friese, J. Enger, H. Rubinsztein-Dunlop, and N. R. Heckenberg, *Phys. Rev. A* **54**, 1593 (1996).
- [13] A. Ashkin, J. M. Dziedzic, J. E. Bjorkholm, and S. Chu, *Opt. Lett.* **11**, 288 (1986).
- [14] J. E. Curtis, B. A. Koss, and D. G. Grier, *Opt. Comm.* **207**, 169 (2002).
- [15] M. Born and E. Wolf, *Principles of Optics* (Cambridge University Press, Cambridge, 1999), 7th ed.
- [16] C. Pozrikidis, *Boundary Integral and Singularity Methods for Linearized Viscous Flow* (Cambridge University Press, New York, 1992).
- [17] J. R. Blake, *Proc. Cambridge Phil. Soc.* **70**, 303 (1971).
- [18] N. Liron and S. Mochon, *J. Eng. Math.* **10**, 287 (1976).
- [19] E. R. Dufresne, D. Altman, and D. G. Grier, *Europhys. Lett.* **53**, 264 (2001).
- [20] J. Arlt, V. Garces-Chavez, W. Sibbett, and K. Dholakia, *Opt. Comm.* **197**, 239 (2001).
- [21] V. Garces-Chavez, D. McGloin, H. Melville, W. Sibbett, and K. Dholakia, *Nature* **419**, 145 (2002).